MR. DANILO ALMEIDA (Orcid ID : 0000-0002-8747-0085)

Article type   : Original Article

Corresponding author mail id: daniloflorestas@gmail.com

DETECTING SUCCESSIONAL CHANGES IN TROPICAL FOREST STRUCTURE USING GATOREYE DRONE-BORNE LIDAR

Danilo Roberti Alves de Almeida [1,2]; Angelica Maria Almeyda Zambrano [3]; Eben North Broadbent [2]; Amanda L. Wendt[4,5]; Paul Foster[6,7]; Benjamin E. Wilkinson [8]; Carl Salk[9]; Daniel de Almeida Papa[10]; Scott Christopher Stark[11]; Ruben Valbuena[12]; Eric Bastos Gorgens[13]; Carlos Alberto Silva[14,15]; Pedro Henrique Santin Brancalion[1]; Matthew Fagan[16]; Paula Meli[1,17]; Robin Chazdon[18,19]

[1] Department of Forest Sciences, "Luiz de Queiroz" College of Agriculture, University of São Paulo (USP/ESALQ), Piracicaba, SP, Brazil

[2] Spatial Ecology and Conservation Lab, School of Forest Resources and Conservation, University of Florida, Gainesville, FL, USA

[3] Spatial Ecology and Conservation Lab, Department of Tourism, Recreation and Sport Management, University of Florida, Gainesville, FL, USA

[4] Organization for Tropical Studies, San Pedro, Costa Rica

[5] EARTH University, Guácimo, Costa Rica

[6] Reserva Ecológica Bijagual, Sarapiquí, Costa Rica

[7] Department of Ecology and Evolutionary Biology, University of Michigan, Ann Arbor, MI, USA

[8] Geomatics Program, School of Forest Resources and Conservation, University of Florida, Gainesville, FL, USA

[9] University of Agricultural Sciences, Alnarp, Sweden

[10] Embrapa Acre, Rio Branco, Acre, Brazil

[11] Department of Forestry, Michigan State University, East Lansing, MI, USA

[12] School of Natural Sciences, Bangor University, Bangor, UK

[13] Department of Forestry, Federal University of Jequitinhonha e Mucuri Valleys (UFVJM), Diamantina, MG, Brazil

[14] School of Forest Resources and Conservation, University of Florida, Gainesville, FL 32611 USA

[15] Department of Geographical Sciences, University of Maryland, College Park, Maryland, MD 20740, USA

[16] University of Maryland, Baltimore County, MD, USA

[17] Department of Forest Sciences, Universidad de La Frontera, Temuco, Chile

[18] Department of Ecology & Evolutionary Biology, University of Connecticut, Storrs, CT, USA

[19] Tropical Forests and People Research Centre, University of the Sunshine Coast, Sippy Downs, Queensland, Australia

Abstract

Drone-based remote sensing is a promising new technology that combines the benefits of ground-based and satellite-derived forest monitoring by collecting fine-scale data over relatively large areas in a cost-effective manner. Here, we explore the potential of the GatorEye drone-lidar system to monitor tropical forest succession by canopy structural attributes including canopy height, spatial heterogeneity, gap fraction, leaf area density (LAD) vertical distribution, canopy Shannon index (an index of LAD), leaf area index (LAI), and understory LAI. We focus on these variables' relationship to aboveground biomass (AGB) stocks and species diversity. In the Caribbean lowlands of northeastern Costa Rica, we analyze nine tropical forests stands (seven second-growth and two old-growth). Stands were relatively homogenous in terms of canopy height and spatial heterogeneity, but not in their gap fraction. Neither species density or tree community Shannon diversity index were significantly correlated with the canopy Shannon index. Canopy height, LAI, and AGB did not show a clear pattern as a function of forest age. However, gap fraction and spatial heterogeneity increased with forest age, whereas understory LAI decreased with forest age. Canopy height was strongly correlated with AGB. The heterogeneous mosaic created by successional forest patches across human-managed tropical landscapes can now be better characterized. Drone-lidar systems offer the opportunity to improve assessment of forest recovery and develop general mechanistic carbon sequestration models that can be rapidly deployed to specific sites, an essential step for monitoring progress within the UN Decade on Ecosystem Restoration.

1.   Introduction

Most forest cover in human-modified tropical landscapes is now second-growth emerging from former agro-pastoral lands (Chazdon, 2014). Under suitable conditions, tropical forest regrowth reduces the need for extensive active restoration interventions, supports local biodiversity, and enhances landscape functionality by supplying multiple ecosystem goods and services (Brancalion & Chazdon 2017; Chazdon, 2017; Chazdon et al., 2020). Natural regeneration of forest has been a proven, cost-effective approach to expand forest cover in landscape restoration initiatives (Lewis et

al., 2019). In Guanacaste Province, Costa Rica, forest cover increased from 24% to 51% from 1986–2012 due to forest succession on abandoned pastures (Calvo et al., 2019). Similarly, in Brazil's Atlantic Forest region, 2.7 M ha regenerated naturally from 1996-2015, contributing 8% of current forest cover (Crouzeilles et al., 2020). Increasing areas covered by second-growth forest can be an indicator of restoration outcomes under favorable conditions (Chazdon & Guariguata, 2016). However, second-growth forest patches differ in age, size, soil type, distance to seed sources, land use, and disturbance histories (e.g., fire, cattle grazing, logging) (Arroyo-Rodríguez et al., 2016; Crouzeilles et al., 2016). Tree cover established by second-growth forests in agricultural landscapes is, in fact, a heterogeneous mosaic of patches varying in biomass, diversity, and species composition (Solar et al., 2015; Poorter et al., 2016; Rozendaal et al., 2019).

The early stages of forest succession in tropical rain forests are dominated by low-stature pioneer trees with a relatively homogeneous canopy cover and dense understory vegetation (Nicotra et al., 1999, Montgomery & Chazdon, 2001). After several decades, late-successional trees dominate most strata of the forest, and forest biomass concentrates in large, often emergent, individuals that increase the complexity of the vertical structure of the forest (Ruiz-Jaen & Potvin, 2011). While successional changes in canopy structural attributes (CSA) such as height, openness, leaf area, and architecture have received attention in forest ecological studies (Stark et al., 2012, 2015; Chanthorn et al., 2016), relatively little is known about the complex interrelationship between the development of these attributes and forest recovery trajectories. Furthermore, these attributes likely have key impacts on forest function — how regenerating forests use nutrients, light, and water — as they age (Scheuermann et al., 2018), and may impact forest sensitivity to disturbances related to global climate change, such as severe, prolonged drought (Laurance, 2004).

The methods currently used to monitor tropical forest succession are based on labor-intensive inventory field plots that rarely cover more than a few hectares. Relative to the millions of hectares in the tropics undergoing regrowth (Crouzeilles et al., 2019; Nanni et al., 2019), plot-based monitoring is a limited (though valuable for certain purposes) approach, particularly given the challenge of accessing remote regions. While detailed ground-based measurements remain the gold standard for measuring species diversity and carbon storage, remote sensing approaches are beginning to offer complementary advantages even at the plot-scale, such as the ability to measure structural attributes like leaf area index and canopy height, without the need for destructive sampling (Calders et al., 2015). Remote sensing approaches based on satellite imagery have been used to map forest regeneration (Hansen et al., 2013; Almeida et al., 2019a), but the coarse spatial resolution and 2D images limits their utility to monitor successional change or meaningfully

differentiate among tree cover types (e.g., natural regeneration vs. monoculture plantations) that are finely interwoven in mosaic landscapes (Hickey et al., 2019).

Active remote sensor lidar (light detection and ranging), in particular, is the best option for measuring three-dimensional structural parameters of the forest canopy (Almeida et al., 2019a). Lidar emits hundreds of thousands of electromagnetic waves per second in the near-infrared (~900 nm wave-length). These pulses hit forest targets (ground, branches, and leaves), and, by analyzing the time delay from pulse emission to return, makes it possible to build an accurate three-dimensional model of the forest. One of the main advantages of this system is that some pulses can penetrate the forest canopy, recording information about the subcanopy, understory, and ground vegetation. Thus, lidar delivers a three-dimensional cloud of points that represent the physical structure of the forest. Successional changes could be characterized using lidar-derived metrics such as mean canopy height, gap fraction, and leaf area, enabling robust monitoring of both forest development and degradation (Caughlin et al., 2016; Almeida et al., 2019b).

Drone-based remote sensing is a promising new technology that provides fine-scale data over relatively large areas (hundreds and thousands of hectares) at a relatively low cost (Anderson et al., 2013; Zahawi et al., 2015). However, typical vegetation indices (e.g., NDVI), derived from multispectral imaging optical sensors, saturate in dense forests (Turner et al., 1999) and do not offer clear information about the detailed structural configuration of the canopy. Because lidar systems can penetrate the canopy, they provide detailed information on vegetation beneath the forest canopy, as well as general information about forest height and spatial arrangement of leaf area (Almeida et al., 2019c).

The application of drone-borne lidar data for monitoring restoration remains poorly explored and underdeveloped relative to its potential to reveal detailed functional and ecological information about the drivers of structure and function in regenerating tropical forests. Drone-borne lidar could significantly advance and broaden the monitoring of forest regeneration (Almeida et al., 2019c), particularly in tropical regions where multiple ambitious restoration commitments have been recently established in an effort to mitigate climate change and conserve biodiversity (Brancalion et al., 2019). Here, we explore the potential of a drone-borne lidar system (GatorEye Unmanned Flying Laboratory) to monitor tropical forest succession by assessing canopy structural attributes, which are otherwise difficult to measure with traditional forest inventories. We also investigate the relationships between canopy structural attributes and aboveground biomass and species diversity.

2.   Material and methods

2.1. Study Area

The study was conducted in nine forested plots in Sarapiquí, Heredia Province, in the Caribbean lowlands (50-220 m a.s.l.) of northeastern Costa Rica (Table 1; Figure 1). Mean annual rainfall is 3800 mm, and mean annual temperature is 26°C at the nearby La Selva Biological Station (McDade et al., 1994); the natural vegetation is classified as Tropical Moist Forest (sensu Holdridge et al., 1975). Soils are derived from weathered basalt and are classified as ultisols (Sollins et al., 1994). All plots are located in a landscape consisting of second- and old-growth forest patches immersed in a matrix of pastures and agricultural fields. Seven plots are in stands between 22 and 45 yrs old, and two others are in a nearby old-growth forest (>100 yr). All second-growth forest plots were previously used for pasture. Many studies of forest succession have been previously published using these plots (Chazdon et al., 2005; 2006; 2010; Dubayah et al., 2010; Becknell et al., 2018).

2.2. Field data collection

Five of the study plots were established in 1997 (LEPS, CR1, CR2, TIR, and LSUR; see Table 1), and four were established in 2006 (JE, FEB, SV, and LEPP; see Table 1). In each plot, all trees ≥ 5 cm in diameter at breast height (DBH) were tagged, mapped, identified, and measured within 10×10 m subplots. DBH was measured at 1.3 m height or above stem anomalies (buttresses or stilt roots; ladders were used when needed). Vouchers were collected for identification and compared with specimens in the La Selva Herbarium. Every year through 2017, the plots were remeasured, and new recruits were tagged, measured, and identified.

2.3. Drone lidar data collection

Plots were overflown using the GatorEye Unmanned Flying Laboratory over the course of two weeks in August 2017. The sensor suite was comprised of a Phoenix Scout system (hardware system that integrates lidar and other sensors with inertial and georeferencing systems to data collection and preparing), a Velodyne VLP-16 Puck Lite laser scanner (lidar sensor), an onboard single-antenna global navigation satellite system (GNSS) receiver (that performs georeferencing of data), and a STIM300 inertial measurement unit (IMU) (which measures the drone's multi-directional movements and orientation, and assists in increasing the accuracy of data

georeferencing). A ground base station X900S-OPUS GNSS receiver collected static GNSS data during the flight, which were used to calculate a post-processed kinematic (PPK) trajectory via Novatel Inertial Explorer software (which enables the high accuracy and precision of data geolocation). More details can be found at the GatorEye website (www.gatoreye.org). Absolute point accuracy has been tested using ground-surveyed checkpoints, showing a root mean square error (RMSE) of 5 cm (Wilkinson et al., 2019). The autonomous flight was programmed to take place at a speed of 8 m/s at 60 m above ground. The transects were spaced 15 meters apart (Figure 2), producing a high-density point cloud (458 ± 170 pts.m^{-2}; mean$\pm SD$).

2.4.   Data processing and analysis

We filtered the drone-derived lidar point clouds to eliminate spurious returns, as described by Almeida et al. (2019c). A digital terrain model (DTM) with 0.5 m resolution was created for each site from the interpolation of ground returns. The algorithm by Zhang et al. (2016) was used for ground classification, as implemented in the "lidR" package of R (Roussel et al., 2019). This DTM was used to normalize the drone-lidar point cloud (i.e., calculate heights above ground), and also to interpolate a canopy height model (CHM) with 0.5-m resolution. The CHM and normalized lidar point clouds were clipped based on the polygons of the georeferenced field plots. The four corners of each rectangular plot were georeferenced using a handheld Garmin 60x GNSS unit (2 m precision through waypoint averaging).

From the normalized point clouds at each plot, we computed the leaf area density (LAD) profiles and leaf area index (LAI). The LAD is the area of leaves found in one unit of canopy volume. It can be seen as the decomposition of the LAI among the vertical strata of the forest canopy (more details in Almeida et al., 2019d). We computed LAD and LAI based on the MacArthur-Horn equation (MacArthur & Horn, 1969) as described in Almeida et al. (2019d). This method provides a basis to estimate variation in vegetation density from optical transmission rates. LAD profiles were calculated from 1 m above the ground (to avoid possible ground returns - lidar cloud points that represent the ground but can be erroneously quantified as vegetation), using 4 m^3 voxels (three-dimensional pixels). The voxels had 2×2 m horizontal resolution and 1 m vertical resolution. Only first returns within 5° of the scan nadir view angle were considered in the computation. We fixed K = 1 (MacArthur-Horn equation; see details in Almeida et al., 2019d) to calculate the "effective LAD" and "effective LAI", which are hereafter referred to as simply LAD

and LAI, for convenience. At each plot, LAI was calculated as the sum of LAD values obtained along with the profile. For visual comparisons, we also calculated a mean leaf area density (LAD, $m^2 \ m^{-3}$) profile of all the LAD profiles calculated within each plot. We also carried out a forest gap analysis from the CHM (Silva et al., 2019) to compute the gap fraction. We considered as a forest gap any group of pixels with a height lower than 5 m and an area of at least 10 m^2 (see also Stark et al., 2012).

Six canopy structural attributes (CSA) were derived from the lidar data: three from the CHM and three from the normalized cloud. For each plot, we computed: (i) canopy height (mean of the CHM); (ii) gap fraction (proportion of area with gaps); (iii) spatial heterogeneity (CHM standard deviation); (iv) leaf area index (sum of LAD); (v) understory LAI (LAI$_{understory}$; the sum of LAD between 1–5 m above the ground); (vi) the leaf area height volume (LAHV, Eq. 1). LAHV was calculated as the sum of the products of height and mean LAD at that height, for each of the 1 m height intervals i in the LAD profile. LAHV was introduced for the first time in Almeida et al. (2019b), who found that LAHV has the potential to estimate forest biomass in forests with different allometric relationships (i.e., height and AGB ratio). Biologically, the assumptions are that leaf area and basal area are directly proportional, while cross-sectional area of branches are approximately constant over branching generations, and the number of branching generations increases linearly with height (West et al., 1997). Thus, LAHV is positively correlated with forest AGB (see the model in Stark et al., 2015).

$$LAHV = \sum(i \times LAD_i) \tag{1}$$

where i (i = 1, 2, 3, …, maximum height) is the height within the canopy, and LAD_i is the horizontal mean of leaf area densities at that respective height (Figure 3).

Using the data measured in the field (inventory data of all trees with DBH $\geq$ 5 cm), we calculated the aboveground dry woody biomass (*agb*, in kg) of each tree, using the formula of Chave et al. (2014):

$$agb = \exp(-1.803 - 0.976*E + 0.976*\ln(wd) + 2.673*\ln(d) - 0.0299*[\ln(d)]^2) \tag{2}$$

where E is a measure of environmental stress, wd is the species-specific wood density, and d is the DBH of each tree. The E coefficient for the study area (E = -0.0625) was obtained using the *retrieve_raster* function developed by Rejou-Mechain & Chave (2014) for accessing their datasets in R (R Core Team 2019). Wood density data were collected from trees within the plots (Plourde et al., 2015). For species with no local wood density data, values from the "Global Wood Density Database" (Zanne et al., 2009) were used. For each plot, we totaled the *agb* of all trees to calculate the density of aboveground biomass (AGB, in Mg·ha^{-1}) in that forest area.

We related the six CSAs and the estimated AGB to forest age using a linear model (for gap fraction and spatial heterogeneity, Eq. 3) or an exponential model (for AGB, canopy height, LAI, and LAI understory, Eq. 4):

$$CSA = \beta_0 + \beta_1 \, Age \qquad (3)$$

where β_0 and β_1 are the intercept and slope of the model, respectively.

$$CSA = \alpha + (\beta - \alpha) \, exp \left(\frac{-(Age)}{\gamma} \right) \qquad (4)$$

where *alpha* is the asymptote of the model representing CSA, *betha* is the intercept of the model, and *gamma* is related to the rate of change in CSA with increasing age. The model was fit with a nonlinear least-squares method, and its significance tested with a Fisher's test. Assuming that 100 years would be enough to reach forest structural maturity, the old-growth forests were assigned an age of 100 years for all analyses involving age (Guariguata et al., 1997). To identify and eliminate outliers, we used *t*-tests based on studentized residuals implemented using the function *outlier.test* in R package "car" (Fox and Weisberg 2011).

We further estimated AGB from lidar-derived canopy height, gap fraction, spatial heterogeneity, and LAHV using ordinary least squares linear regression. The assessment of model accuracy was performed by a leave-one-out cross-validation (LOOCV) procedure, which re-calculates the model for each set of n-1 observations and uses that model to predict the omitted observation. The relationship between the observed (measured) and predicted (via LOOCV) values was evaluated by testing their 1:1 correspondence under the null hypothesis that their regression intercept and slope were 0 and 1 respectively (Valbuena et al., 2017).

Finally, we examined the relationship between tree species diversity and forest structure. We considered two measures of tree species diversity: (1) species density (number of species per area using a fixed area); and (2) tree community Shannon diversity index (entropy of species' proportional stem-wise abundances). The potential of lidar to provide a proxy for tree diversity was examined with an additional variable, the structure-based "canopy Shannon index", based on the mean LAD profile of a plot (Stark et al., 2012; Valbuena et al., 2012). The canopy Shannon Index increases with the number of heights having vegetation present and with the equitability of LAD among those vegetated heights (see more details in Almeida et al., 2019b). Spearman correlations were calculated for the canopy Shannon index as a function of each of these two aspects of tree biodiversity.

3.   Results

3.1. Canopy structural attributes and forest age

Canopy structural attributes differed in their between-plot coefficients of variation (CV) (Table 2). Plots were relatively homogenous in terms of canopy height (10.6%) and spatial heterogeneity (26.2%) but not in their gap fraction (100.1%). In fact, the gap fraction was the structural attribute that showed the highest variability among plots, ranging between 0.0% and 3.9%. LAI was, on average 7.24 ± 0.36 (mean$\pm$SD) (Table 2), and all plots had an LAI between 6.6 and 7.6 (Figure 3). However, each plot showed a distinct LAD profile (Figure 3). In general, LAI varied among plots (CV=5%), and was more variable in the understory (CV=23.7%) (Table 2).

Gap fraction ($r^2 = 0.72$, $p = 0.008$), and spatial heterogeneity ($r^2 = 0.83$, $p = 0.002$) were positively associated with forest age, while LAI$_{understory}$ was negatively associated with forest age ($r^2 = 0.52$, $p = 0.045$; Figure 4). However, none of these variations showed a significant correlation when the two old-growth plots were eliminated from the regression (p-values > 0.005). LAI, AGB, and canopy height did not show any pattern with forest age (Figure 5). In our analysis, the old-growth forests were assigned an age of 100 years (enough to reach the forest's structural maturity); however, the results were similar when we performed the analysis with a 200 year forest maturity value.

3.2. Predicting biomass and diversity

Canopy height (lidar-derived) significantly predicted AGB ($r^2 = 0.80$, $p = 0.001$, Figure 6). LAHV, gap fraction and spatial heterogeneity showed no significant linear correlation with AGB (Figure S1). Neither species density nor tree community Shannon diversity index were significantly correlated (Spearman correlation) with lidar-derived canopy Shannon index ($p = 0.168$ and $p = 0.385$, respectively; Figure S2).

4. Discussion

Our study demonstrates the potential of drone-borne lidar to assess the structure and biomass of tropical forests at different successional stages. To our knowledge, this is the first study to use this technology to study or monitor tropical forest succession. Forest age was positively correlated with spatial heterogeneity and gap fraction, and negatively with understory LAI. The accuracy of AGB estimates from lidar-derived variables (canopy height and LAHV) was high and supports other reports considering primary and disturbed tropical forests (Longo et al., 2016). The canopy structure attributes observed with lidar were not clearly related to taxonomic diversity but may be related to

forest structure and function variables necessary for monitoring forest recovery. Below, we briefly review these likely connections to highlight frontiers for further exploring the capacity of lidar to monitor successional changes in forest structure, function, and ecosystem services.

4.1. Canopy structural attributes and forest age

Previous studies have investigated the use of drone-borne lidar systems in restoration plantations in the Brazilian Atlantic Forest (Almeida et al. 2019c) and in natural forests in Arizona (Sankey et al. 2017). For the first time, this study describes canopy structural attributes and foliage-height profiles for a series of nine tropical forest plots with a range of ages, allowing a quantitative analysis of successional changes in structure. Almeida et al. (2019c), also using the GatorEye system, found LAD profiles with a monomodal shape (leaf area concentrated in a single vertical stratum) in forest restoration plantations in Brazil's Atlantic Forest. This monomodal pattern seems to be characteristic of relatively young even-aged plantations (less than 20 years old), even when the species are highly diverse (Almeida et al., 2019b). The natural regeneration studied here showed a LAD with more evenly distributed vegetation along the vertical profile (i.e., without a concentration of lidar returns at any given height), or with multiple peaks corresponding to vegetation stratification (Figure 3). This characteristic appears to be more typical of old-growth forests, or advanced stages of natural regeneration, and likely results from the development of an uneven age structure related to natural establishment and gap formation and closure dynamics (occupying multiple vertical positions in the canopy) (Stark et al., 2012; Valbuena et al., 2012; Almeida et al., 2016, 2019b).

The decline of understory LAI in old-growth forests has also been observed in other studies (Almeida et al., 2019b). This pattern is clearly driven by the old-growth forest data. These results are consistent with theories of competition for light in tropical forests, which show that recruitment declines due to growth of smaller trees into the intermediate canopy strata and the closure of the upper canopy (Rüger et al., 2009). For example, while carrying out field inventories for this study, it was clear that the understory of old-growth forests are much easier to walk through than in second-growth forests, in agreement with the lidar results. Metrics of light transmission, with varying degrees of realism, can also be modeled from vegetation profiles to help explain forest successional dynamics (Stark et al., 2012). In the same study area featured here, Montgomery & Chazdon (2001), found that understory (one to four meters high) light availability was higher in old-growth than in 15-20 yr old second-growth forests, and was reduced in second-growth forests by the higher density of saplings and shrubs.

Forest canopy variables are fundamental to understanding many ecological processes. Forest structure, including foliage density, canopy cover, and stratification, influence light availability and consequently affect light use and ecosystem productivity (Nicotra et al., 1999; Montgomery & Chazdon, 2001; Ishii et al., 2004). The quantity and distribution of foliage drive the rates of energy, water, and nutrient flux, which are directly related to forest succession (Feldpausch 2005). Differences in vertical and horizontal distribution of LAD may provide insights into the relationship between tree LAI and ecosystem functions, especially hydrological processes such as water storage (Lorens & Gallart 2000; Keim & Link 2018) and kinetic energy dissipation of raindrops (Geißler et al., 2013; Song et al., 2018).

Not all forest canopy variables in our study showed clear age-related trends. Differences in AGB, canopy height, and LAI across sites were not explained by stand age. We believe the cause for this is that the youngest forests in this study were already 22 years old, which is sufficient time for significant structural and biomass formation. Furthermore, the presence of larger remnant trees within some of the second-growth forests may have obscured the effects of stand age in the chronosequence analysis (Chazdon et al., 2014). Becknell et al. (2018), using airborne lidar, showed that chronosequence results are robust at the landscape scale, and the sample area required to produce estimates of canopy height and AGB approximating the landscape-scale mean is larger than the typical area sampled in second-growth forest chronosequence studies. The relationship between forest age and AGB is apparent when we analyze long-term changes within each plot (Figure S3). Regression results support ground-level research in the same study area that concluded that old-growth forests have a higher gap fraction and spatial heterogeneity than young second-growth forests (Nicotra et al., 1999; Montgomery & Chazdon, 2001). Nicotra et al. (1999) in the same study area, found that 15-20 yr old second-growth forest canopies are more homogeneous (or have less gap) than old-growth canopies. Another study using lidar measurements also found higher spatial heterogeneity in old-growth forests than in second-growth forests in the Brazilian Atlantic Forest biome (Almeida et al., 2019b).

One of the main limitations of the present study is the low number of samples (nine plots), which limits model development and testing. A valuable approach would be to use a much larger set of plots and try to develop more complex models using multivariate regression or machine learning (Valbuena et al., 2016). In addition, we found outliers in some models. The outlier found for gap fraction, spatial heterogeneity, and understory LAI corresponds to the 35-yr old "Tirimbina" plot. The lidar point cloud for this plot (Figure S4) shows large gaps (and consequent higher spatial heterogeneity and understory LAI), when compared, for example, with the similarly aged (40 yrs.)

"LEP Secondary" plot. These gaps are caused by the mortality of large-crowned canopy trees of *Vochysia ferruginea*, that dominate this plot.

4.2. Predicting biomass and species diversity

In our analysis, AGB was well explained by canopy height, in agreement with many previous studies (e.g., Longo et al., 2016; Valbuena et al., 2017; Almeida et al., 2019c, 2019e). Here, the LAHV, did not significantly improve AGB prediction. This likely happened because we analyzed one forest type only, and for this forest type, the allometric relationship between AGB and canopy height did not show much variation. Almeida et al. (2019b), however, found great potential of LAHV in AGB prediction when comparing forest types with greater structural differences (old- and second-growth forests, monoculture plantations, and high-diversity plantations).

In this study, we failed to find significant relationships between tree species density and canopy structure measures. While Almeida et al. (2019b) found a weak relationship between the canopy Shannon index and the tree species Shannon index, the canopy complexity of second- and old-growth tropical forests seems to saturate at a relatively low species density. Other studies have shown the combination of lidar and hyperspectral data to be a promising path to assess tree diversity (Asner et al., 2015; Sankey et al., 2017). Due to the difficulty and complexity of finding clear relationships between canopy structures (and their possible combinations) with diversity, new machine learning tools (Valbuena et al., 2016) could be good alternatives for exploring these relationships and creating efficient models. However, these approaches usually require a relatively high number of samples (many more than we have in the present study). Most studies of second-growth forests are based on much smaller plots and have larger sample sizes when compared to the present study. It is not clear what the best spatial scale is to detect these relationships. In the same study plots featured here, Lasky et al. (2014) found that the relationship between species richness and biomass change was not significant in the mid-successional and old-growth stands when 100 m^2 quadrats were sampled.

4.3. Implications for monitoring tropical forest succession using drone-borne lidar systems

Canopy structural metrics are important attributes that may evince forest changes through time. Our findings provide insights into forest structure development and ecological processes occurring in the naturally regenerating forests. Other links between forest structure and function could be derived directly from combining the three-dimensional data opening new opportunities for mapping more

complex variables such as leaf chlorophyll and N content, and even ecosystem functions such as photosynthetic performance (Eitel et al., 2010, 2011; Magney et al., 2014). In this way, lidar could provide meaningful information for developing ecological models and forest change monitoring, in both naturally regenerated and planted forests. As a high resolution, non-destructive, and efficient tool, lidar systems are increasingly applied for reliable three-dimensional data acquisition and comparison in forest inventories (Song et al., 2018).

We highlight the usefulness of drone-based lidar to monitor and estimate the structural parameters of trees from the forest stand level to landscape with three-dimensional structure information (Asner et al., 2011, Baccini et al., 2012). Our field data came from a long-term study of tropical forest succession in wet lowland forests of Costa Rica (Chazdon et al., 2010), so it would not necessarily be suitable for calibrating lidar-derived biomass calculations in other regions. Field data required to calibrate models of lidar-derived biomass estimates may be available for other regions or forest types. In this sense, we need systematic analyses bringing together lidar data from plots around the world, across degradation gradients to see what patterns emerge when we include more complete data.

Despite the great practicality and autonomy that drone systems provide, the price and accessibility of complex systems with lidar and hyperspectral sensors are still limited. Drone-lidar and drone-lidar-hyperspectral systems still have very high prices (~ US $ 100,000 - US $ 450,000; The GatorEye falls within that range) when compared to drone systems with conventional RGB (red, green and blue channels) cameras (~ US $ 1,500). However, we expect that this type of technology will become much less expensive in the coming years. Also, it is necessary to keep in mind that these systems are quite fragile and require a high degree of technical knowledge for their operation. However, 3D photogrammetry techniques (a.k.a. Structure from Motion) (Cruzan et al., 2016; Swinfield et al., 2019) make it possible to obtain highly accurate digital surface models. However, this technique has two major limitations: the first is the high computational cost for processing 3D photogrammetry data. Most commercial structure from motion software companies (e.g., Pix4D and Dronedeploy) now have these processing features through cloud-based computing and at a reasonable cost. That greatly reduces the need to have powerful desktop computers, as images are essentially uploaded in batches and processed remotely. The second is that this technique cannot calculate leaf area density profiles and the ground elevation below the forest (like lidar does). Therefore, to calculate the canopy height, it is necessary to have a priori knowledge of the ground elevation (Zahawi et al., 2015).

International accords, such as the Paris Agreement on climate change and the Convention on Biological Diversity, require reporting aspects of forest structure and health, including for forests

outside of protected areas. But there is also an urgent need to track and monitor forest recovery not just for carbon sequestration but also for other significant benefits, such as biodiversity, water recharge, and evapotranspiration (Bryan et al., 2015; Chazdon et al., 2016; Mukul et al., 2016). Drone-borne lidar data opens up the possibility of replacing intermittently measured field plots (e.g., bigplotnetwork.org), guesswork, and general models with site-specific and up-to-date data, and offer a critical contribution for the 2021-2030 United Nations Decade on Ecosystem Restoration.

DATA AVAILABILITY

Data available from Zenodo https://zenodo.org/record/3765329#.XqbhB2hKjIU and https://zenodo.org/record/3779950#.Xqv8uKhKjIU

References

Almeida, D. R. A., B. W. Nelson, J. Schietti, E. B. Gorgens, A. F. Resende, S. C. Stark, and R. Valbuena. 2016. Contrasting fire damage and fire susceptibility between seasonally flooded forest and upland forest in the Central Amazon using portable profiling LiDAR. Remote Sensing of Environment 184:153–160.

Almeida, D. R. A., S. C. Stark, R. Valbuena, E. N. Broadbent, T. S. F. Silva, A. F. Resende, M. P. Ferreira, A. Cardil, C. A. Silva, N. Amazonas, A. M. A. Zambrano, and P. H. S. Brancalion. 2019a. A new era in forest restoration monitoring. Restoration Ecology.

Almeida, D. R. A., S. C. Stark, R. Chazdon, B. W. Nelson, R. G. Cesar, P. Meli, E. B. Gorgens, M. M. Duarte, R. Valbuena, V. S. Moreno, A. F. Mendes, N. Amazonas, N. B. Gonçalves, C.

A. Silva, J. Schietti, and P. H. S. Brancalion. 2019b. The effectiveness of lidar remote sensing for monitoring forest cover attributes and landscape restoration. Forest Ecology and Management 438:34–43.

Almeida, D. R. A., E. N. Broadbent, A. M. A. Zambrano, B. E. Wilkinson, M. E. Ferreira, R. Chazdon, P. Meli, E. B. Gorgens, C. A. Silva, S. C. Stark, R. Valbuena, D. A. Papa, and P. H. S. Brancalion. 2019c. Monitoring the structure of forest restoration plantations with a drone-lidar system. International Journal of Applied Earth Observation and Geoinformation 79:192–198.

Almeida, D. R. A. de, S. C. Stark, G. Shao, J. Schietti, B. W. Nelson, C. A. Silva, E. B. Gorgens, R. Valbuena, D. de A. Papa, and P. H. S. Brancalion. 2019d. Optimizing the Remote Detection of Tropical Rainforest Structure with Airborne Lidar: Leaf Area Profile Sensitivity to Pulse Density and Spatial Sampling. Remote sensing 11:92.

Almeida, D. R. A., S. C. Stark, J. Schietti, J. L. C. Camargo, N. T. Amazonas, E. B. Gorgens, D. M. Rosa, M. N. Smith, R. Valbuena, S. Saleska, A. Andrade, R. Mesquita, S. G. Laurance, W. F. Laurance, T. E. Lovejoy, E. N. Broadbent, Y. E. Shimabukuro, G. G. Parker, M. Lefsky, C. A. Silva, and P. H. S. Brancalion. 2019e. Persistent effects of fragmentation on tropical rainforest canopy structure after 20 yr of isolation. Ecological Applications 29:e01952.

Anderson, K., and K. J. Gaston. 2013. Lightweight unmanned aerial vehicles will revolutionize spatial ecology. Frontiers in Ecology and the Environment 11:138–146.

Arroyo-Rodríguez, V., F. P. L. Melo, M. Martínez-Ramos, F. Bongers, R. L. Chazdon, J. A. Meave, N. Norden, B. A. Santos, I. R. Leal, and M. Tabarelli. 2017. Multiple successional pathways in human-modified tropical landscapes: new insights from forest succession, forest fragmentation and landscape ecology research. Biological Reviews of the Cambridge Philosophical Society 92:326–340.

Asner, G. P., S. L. Ustin, P. A. Townsend, R. E. Martin, and K. D. Chadwick. 2015. Forest biophysical and biochemical properties from hyperspectral and LiDAR remote sensing. L. Resour. Monit. Model. Mapp. with Remote sensing. CRC Press. Taylor Fr. Gr. 429–448.

Baccini, A., S. Goetz, W. Walker, N. Laporte, M. Sun, D. Sulla-Menashe, J. Hackler, P. Beck, R. Dubayah, M. Friedl, S. Samanta, and R. Houghton. 2012. Estimated carbon dioxide emissions from tropical deforestation improved by carbon-density maps. Nature climate change 2:182–185.

Becknell, J. M., S. Porder, S. Hancock, R. L. Chazdon, M. A. Hofton, J. B. Blair, and J. R. Kellner. 2018. Chronosequence predictions are robust in a Neotropical secondary forest, but plots miss the mark. Global change biology 24:933–943.

Brancalion, P. H. S., and R. L. Chazdon. 2017. Beyond hectares: four principles to guide reforestation in the context of tropical forest and landscape restoration. Restoration Ecology 25:491–496.

Brancalion, P. H. S., A. Niamir, E. Broadbent, R. Crouzeilles, F. S. M. Barros, A. M. Almeyda Zambrano, A. Baccini, J. Aronson, S. Goetz, J. L. Reid, B. B. N. Strassburg, S. Wilson, and R. L. Chazdon. 2019. Global restoration opportunities in tropical rainforest landscapes. Science Advances 5:eaav3223.

Bryan, B. A., R. K. Runting, T. Capon, M. P. Perring, S. C. Cunningham, M. E. Kragt, M. Nolan, E. A. Law, A. R. Renwick, S. Eber, R. Christian, and K. A. Wilson. 2015. Designer policy for carbon and biodiversity co-benefits under global change. Nature climate change 6:301–305.

Calders, K., G. Newnham, A. Burt, S. Murphy, P. Raumonen, M. Herold, D. Culvenor, V. Avitabile, M. Disney, J. Armston, and M. Kaasalainen. 2015. Nondestructive estimates of above-ground biomass using terrestrial laser scanning. Methods in ecology and evolution / British Ecological Society 6:198–208.

Calvo-Alvarado, J., Jiménez, V., Calvo-Obando, A., Castillo, M., 2019. Current perspectives on forest recovery trends in Guanacaste, Costa Rica. International Forestry Review 21, 425-431.

Caughlin, T. T., S. W. Rifai, S. J. Graves, G. P. Asner, and S. A. Bohlman. 2016. Integrating LiDAR-derived tree height and Landsat satellite reflectance to estimate forest regrowth in a tropical agricultural landscape. Remote Sensing in Ecology and Conservation 2:190–203.

Chanthorn, W., Y. Ratanapongsai, W. Y. Brockelman, M. A. Allen, C. Favier, and M. A. Dubois. 2016. Viewing tropical forest succession as a three-dimensional dynamical system. Theoretical ecology 9:163–172.

Chave, J., M. Réjou-Méchain, A. Búrquez, E. Chidumayo, M. S. Colgan, W. B. C. Delitti, A. Duque, T. Eid, P. M. Fearnside, R. C. Goodman, M. Henry, A. Martínez-Yrízar, W. A. Mugasha, H. C. Muller-Landau, M. Mencuccini, B. W. Nelson, A. Ngomanda, E. M. Nogueira, E. Ortiz-Malavassi, R. Pélissier, and G. Vieilledent. 2014. Improved allometric models to estimate the aboveground biomass of tropical trees. Global change biology 20:3177–3190.

Chazdon, R. L. 2014. Second growth: the promise of tropical forest regeneration in an age of deforestation. University of Chicago Press.

Chazdon, R. L. 2017. Landscape restoration, natural regeneration, and the forests of the future. Annals of the Missouri Botanical Garden 102:251–257.

Chazdon, R. L., E. N. Broadbent, D. M. A. Rozendaal, F. Bongers, A. M. A. Zambrano, T. M. Aide, P. Balvanera, J. M. Becknell, V. Boukili, P. H. S. Brancalion, D. Craven, J. S. Almeida-Cortez, G. A. L. Cabral, B. de Jong, J. S. Denslow, D. H. Dent, S. J. DeWalt, J. M. Dupuy, S. M. Durán, M. M. Espírito-Santo, and L. Poorter. 2016. Carbon sequestration potential of second-growth forest regeneration in the Latin American tropics. Science Advances 2:e1501639.

Chazdon, R. L., B. Finegan, R. S. Capers, B. Salgado-Negret, F. Casanoves, V. Boukili, and N. Norden. 2010. Composition and Dynamics of Functional Groups of Trees During Tropical Forest Succession in Northeastern Costa Rica. Biotropica 42:31–40.

Chazdon, R. L., and M. R. Guariguata. 2016. Natural regeneration as a tool for large-scale forest restoration in the tropics: prospects and challenges. Biotropica 48:716–730.

Chazdon, R. L., S. G. Letcher, M. van Breugel, M. Martínez-Ramos, F. Bongers, and B. Finegan. 2007. Rates of change in tree communities of secondary Neotropical forests following major disturbances. Philosophical Transactions of the Royal Society of London. Series B, Biological Sciences 362:273–289.

Chazdon, R. L., A. Redondo Brenes, and B. Vilchez Alvarado. 2005. Effects of climate and stand age on annual tree dynamics in tropical second-growth rain forests. Ecology 86:1808–1815.

Chazdon, R.L., Lindenmayer, D., Guariguata, M.R., Crouzeilles, R., Rey Benayas, J.M., Lazos, E., 2020. Fostering natural forest regeneration on former agricultural land through economic and policy interventions. Environmental Research Letters.

Crouzeilles, R., M. Curran, M. S. Ferreira, D. B. Lindenmayer, C. E. V. Grelle, and J. M. Rey Benayas. 2016. A global meta-analysis on the ecological drivers of forest restoration success. Nature Communications 7:11666.

Crouzeilles, R., Beyer, H.L., Monteiro, L.M., Feltran-Barbieri, R., Pessôa, A.C.M., Barros, F.S.M., Lindenmayer, D.B., Lino, E.D.S.M., Grelle, C.E.V., Chazdon, R.L., Matsumoto, M., Rosa, M., Latawiec, A.E., Strassburg, B.B.N., in press. Achieving cost-effective landscape-scale forest restoration through targeted natural regeneration. Conservation Letters in press.

Crouzeilles, R., E. Santiami, M. Rosa, L. Pugliese, P. H. S. Brancalion, R. R. Rodrigues, J. P. Metzger, M. Calmon, C. A. de M. Scaramuzza, M. H. Matsumoto, A. Padovezi, R. de M. Benini, R. B. Chaves, T. Metzker, R. B. Fernandes, F. R. Scarano, J. Schmitt, G. Lui, P. Christ, R. M. Vieira, and S. Pinto. 2019. There is hope for achieving ambitious Atlantic Forest restoration commitments. Perspectives in Ecology and Conservation 17:80–83.

Cruzan, M. B., B. G. Weinstein, M. R. Grasty, B. F. Kohrn, E. C. Hendrickson, T. M. Arredondo, and P. G. Thompson. 2016. Small unmanned aerial vehicles (micro-UAVs, drones) in plant ecology. Applications in plant sciences 4.

Dubayah, R. O., S. L. Sheldon, D. B. Clark, M. A. Hofton, J. B. Blair, G. C. Hurtt, and R. L. Chazdon. 2010. Estimation of tropical forest height and biomass dynamics using lidar remote sensing at La Selva, Costa Rica. Journal of Geophysical Research 115:n/a-n/a.

Eitel, J. U. H., L. A. Vierling, and D. S. Long. 2010. Simultaneous measurements of plant structure and chlorophyll content in broadleaf saplings with a terrestrial laser scanner. Remote Sensing of Environment 114:2229–2237.

Eitel, J. U. H., L. A. Vierling, D. S. Long, and E. R. Hunt. 2011. Early season remote sensing of wheat nitrogen status using a green scanning laser. Agricultural and Forest Meteorology 151:1338–1345.

Fagan, M. E., R. S. DeFries, S. E. Sesnie, J. P. Arroyo, W. Walker, C. Soto, R. L. Chazdon, and A. Sanchun. 2013. Land cover dynamics following a deforestation ban in northern Costa Rica. Environmental Research Letters 8:034017.

Feldpausch, T. R., S. J. Riha, E. C. M. Fernandes, and E. V. Wandelli. 2005. Development of forest structure and leaf area in secondary forests regenerating on abandoned pastures in central amazônia. Earth Interactions 9:1–22.

Fox, J., and S. Weisberg. 2019. An {R} Companion to Applied Regression, Third Edition. Thousand Oaks CA: Sage. URL: https://socialsciences.mcmaster.ca/jfox/Books/Companion/

Geißler, C., K. Nadrowski, P. Kühn, M. Baruffol, H. Bruelheide, B. Schmid, and T. Scholten. 2013. Kinetic energy of Throughfall in subtropical forests of SE China - effects of tree canopy structure, functional traits, and biodiversity. Plos One 8:e49618.

Guariguata, M.R., R. L. Chazdon, J. S. Denslow, J. M. Dupuy, J.M.and L. Anderson. 1997. Structure and floristics of secondary and old-growth forest stands in lowland Costa Rica. Plant Ecology 132: 107-120

Holdridge, L. R., W. G. Grenke, W. H. Haheway, T. Liang, and J. A. Tosi. 1975. Forest environments in tropical life zones. Pergamon Press, New York, New York

Hickey, L. J., J. Atkins, R. T. Fahey, M. T. Kreider, S. B. Wales, and C. M. Gough. 2019. Contrasting development of canopy structure and primary production in planted and naturally regenerated red pine forests. Forests 10:566.

Ishii, H. T., S. I. Tanabe, and T. Hiura.(2004). Exploring the relationships among canopy structure, stand productivity, and biodiversity of temperate forest ecosystems. Forest Science, 50(3), 342-355.

Keim, R. F., and T. E. Link. 2018. Linked spatial variability of throughfall amount and intensity during rainfall in a coniferous forest. Agricultural and Forest Meteorology 248:15–21.

Lasky, J. R., M. Uriarte, V. K. Boukili, D. L. Erickson, W. John Kress, and R. L. Chazdon. 2014. The relationship between tree biodiversity and biomass dynamics changes with tropical forest succession. Ecology Letters 17:1158–1167.

Laurance, W. F. 2004. Forest-climate interactions in fragmented tropical landscapes. Philosophical Transactions of the Royal Society of London. Series B, Biological Sciences 359:345–352.

Lewis, S. L., C. E. Wheeler, E. T. A. Mitchard, and A. Koch. 2019. Restoring natural forests is the best way to remove atmospheric carbon. Nature 568:25–28.

Llorens, P., and F. Gallart. 2000. A simplified method for forest water storage capacity measurement. Journal of hydrology 240:131–144.

Longo, M., M. Keller, M. N. dos-Santos, V. Leitold, E. R. Pinagé, A. Baccini, S. Saatchi, E. M. Nogueira, M. Batistella, and D. C. Morton. 2016. Aboveground biomass variability across intact and degraded forests in the Brazilian Amazon. Global Biogeochemical Cycles 30:1639–1660.

Magney, T. S., S. A. Eusden, J. U. H. Eitel, B. A. Logan, J. Jiang, and L. A. Vierling. 2014. Assessing leaf photoprotective mechanisms using terrestrial LiDAR: towards mapping canopy photosynthetic performance in three dimensions. The New Phytologist 201:344–356.

Montgomery, R. A., and R. L. Chazdon. 2001. Forest structure, canopy architecture, and light transmittance in tropical wet forests. Ecology 82:2707–2718.

Mukul, S. A., J. Herbohn, and J. Firn. 2016. Co-benefits of biodiversity and carbon sequestration from regenerating secondary forests in the Philippine uplands: implications for forest landscape restoration. Biotropica 48:882–889.

McDade, L. A., K. S. Bawa, H. A. Hespenheide, and G. S. Hartshorn (Eds.). (1994). La Selva: ecology and natural history of a neotropical rain forest. University of Chicago Press.

Nanni, A. S., S. Sloan, T. M. Aide, J. Graesser, D. Edwards, and H. R. Grau. 2019. The neotropical reforestation hotspots: A biophysical and socioeconomic typology of contemporary forest expansion. Global Environmental Change 54:148–159.

Nicotra, A. B., R. L. Chazdon, and S. V. B. Iriarte. 1999. Spatial heterogeneity of light and woody seedling regeneration in tropical wet forests. Ecology 80:1908–1926.

Plourde, B. T., V. K. Boukili, and R. L. Chazdon. 2015. Radial changes in wood specific gravity of tropical trees: inter- and intraspecific variation during secondary succession. Functional ecology 29:111–120.

Poorter, L., F. Bongers, T. M. Aide, A. M. Almeyda Zambrano, P. Balvanera, J. M. Becknell, V. Boukili, P. H. S. Brancalion, E. N. Broadbent, R. L. Chazdon, D. Craven, J. S. de Almeida-Cortez, G. A. L. Cabral, B. H. J. de Jong, J. S. Denslow, D. H. Dent, S. J. DeWalt, J. M. Dupuy, S. M. Durán, M. M. Espírito-Santo, and D. M. A. Rozendaal. 2016. Biomass resilience of Neotropical secondary forests. Nature 530:211–214.

R Core Team. 2019. R: A language and environment for statistical computing. R Foundation for Statistical Computing, Vienna, Austria. 692 URL http://www.R-Project.org/.

Réjou-Méchain M., and J. Chave. 2014. Manipulate raster and netCDF datasets. http://chave.ups-tlse.fr/pantropical_allometry/readlayers.r (last accessed October 2019).

Roussel, J., and D. Auty. 2019. lidR: Airborne LiDAR Data Manipulation and Visualization for Forestry Applications. R package version 2.0.0.

Rozendaal, D. M. A., F. Bongers, T. M. Aide, E. Alvarez-Dávila, N. Ascarrunz, P. Balvanera, J. M. Becknell, T. V. Bentos, P. H. S. Brancalion, G. A. L. Cabral, S. Calvo-Rodriguez, J. Chave, R. G. César, R. L. Chazdon, R. Condit, J. S. Dallinga, J. S. de Almeida-Cortez, B. de Jong, A. de Oliveira, J. S. Denslow, and L. Poorter. 2019. Biodiversity recovery of Neotropical secondary forests. Science Advances 5:eaau3114.

Rüger, N., A. Huth, S. P. Hubbell, and R. Condit. 2009. Response of recruitment to light availability across a tropical lowland rain forest community. Journal of Ecology 97:1360–1368.

Ruiz-Jaen, M. C., and C. Potvin. 2011. Can we predict carbon stocks in tropical ecosystems from tree diversity? Comparing species and functional diversity in a plantation and a natural forest. The New Phytologist 189:978–987.

Sankey, T., J. Donager, J. McVay, and J. B. Sankey. 2017. UAV lidar and hyperspectral fusion for forest monitoring in the southwestern USA. Remote Sensing of Environment 195:30–43.

Scheuermann, C. M., L. E. Nave, R. T. Fahey, K. J. Nadelhoffer, and C. M. Gough. 2018. Effects of canopy structure and species diversity on primary production in upper Great Lakes forests. Oecologia 188:405–415.

Silva, C. A., R. Valbuena, E. R. Pinagé, M. Mohan, D. R. A. de Almeida, E. N. Broadbent, W. S. W. M. Jaafar, D. de Almeida Papa, A. Cardil, and C. Klauberg. 2019. ForestGapR: An R Package for Forest Gap Analysis from Canopy Height Models. Methods in ecology and evolution / British Ecological Society.

Solar, R. R. de C., J. Barlow, J. Ferreira, E. Berenguer, A. C. Lees, J. R. Thomson, J. Louzada, M. Maués, N. G. Moura, V. H. F. Oliveira, J. C. M. Chaul, J. H. Schoereder, I. C. G. Vieira, R. Mac Nally, and T. A. Gardner. 2015. How pervasive is biotic homogenization in human-modified tropical forest landscapes? Ecology Letters 18:1108–1118.

Sollins, P., F. Sancho M., R. Mata Ch., and R. L. Jr. Sanford. 1994. Soils and soil process research. In L. A. McDade, K. S. Bawa, H. A. He spenheide, and G. S. Hartshorn (Eds.). La Selva: Ecology and natural history of a neotropical rain forest, pp. 34-53. University of Chicago Press, Chicago, Illinois.

Song, Z., S. Seitz, P. Zhu, P. Goebes, X. Shi, S. Xu, M. Wang, K. Schmidt, and T. Scholten. 2018. Spatial distribution of LAI and its relationship with throughfall kinetic energy of common tree species in a Chinese subtropical forest plantation. Forest Ecology and Management 425:189–195.

Stark, S. C., B. J. Enquist, S. R. Saleska, V. Leitold, J. Schietti, M. Longo, L. F. Alves, P. B. Camargo, and R. C. Oliveira. 2015. Linking canopy leaf area and light environments with tree size distributions to explain Amazon forest demography. Ecology Letters 18:636–645.

Stark, S. C., V. Leitold, J. L. Wu, M. O. Hunter, C. V. de Castilho, F. R. C. Costa, S. M. McMahon, G. G. Parker, M. T. Shimabukuro, M. A. Lefsky, M. Keller, L. F. Alves, J. Schietti, Y. E. Shimabukuro, D. O. Brandão, T. K. Woodcock, N. Higuchi, P. B. de Camargo, R. C. de Oliveira, S. R. Saleska, and J. Chave. 2012. Amazon forest carbon dynamics predicted by profiles of canopy leaf area and light environment. Ecology Letters 15:1406–1414.

Swinfield, T., J. A. Lindsell, J. V. Williams, R. D. Harrison, Agustiono, Habibi, E. Gemita, C. B. Schönlieb, and D. A. Coomes. 2019. Accurate measurement of tropical forest canopy heights and aboveground carbon using structure from motion. Remote sensing 11:928.

Turner, D. P., W. B. Cohen, R. E. Kennedy, K. S. Fassnacht, and J. M. Briggs. 1999. Relationships between Leaf Area Index and Landsat TM Spectral Vegetation Indices across Three Temperate Zone Sites. Remote Sensing of Environment 70:52–68.

Valbuena, R., A. Hernando, J. A. Manzanera, E. B. Görgens, D. R. A. Almeida, F. Mauro, A. García-Abril, and D. A. Coomes. 2017. Enhancing of accuracy assessment for forest above-ground biomass estimates obtained from remote sensing via hypothesis testing and overfitting evaluation. Ecological Modelling 366:15–26.

Valbuena, R., M. Maltamo, and P. Packalen. 2016. Classification of forest development stages from national low-density lidar datasets: a comparison of machine learning methods. Revista de Teledetección:15.

Valbuena, R., P. Packalén, S. Martı́n-Fernández, and M. Maltamo. 2012. Diversity and equitability ordering profiles applied to study forest structure. Forest Ecology and Management 276:185–195.

West, G. B., J. H. Brown, and B. J. Enquist. 1999. The fourth dimension of life: fractal geometry and allometric scaling of organisms. Science 284:1677–1679.

Wilkinson, B., H. A. Lassiter, A. Abd-Elrahman, R. R. Carthy, P. Ifju, E. Broadbent, and N. Grimes. 2019. Geometric targets for UAS lidar. Remote sensing 11:3019.

Zahawi, R. A., J. P. Dandois, K. D. Holl, D. Nadwodny, J. L. Reid, and E. C. Ellis. 2015. Using lightweight unmanned aerial vehicles to monitor tropical forest recovery. Biological Conservation 186:287–295.

Zanne, A. E., G. Lopez-Gonzalez, D. A. Coomes, J. Ilic, S. Jansen, S. L. Lewis, R. B. Miller, N. G. Swenson, M. C. Wiemann, and J. Chave. 2009. Data from: Towards a worldwide wood economics spectrum. Dryad Digital Repository.

Zhang, W., J. Qi, P. Wan, H. Wang, D. Xie, X. Wang, and G. Yan. 2016. An Easy-to-Use Airborne LiDAR Data Filtering Method Based on Cloth Simulation. Remote sensing 8:501.

Tables

Table 1. Descriptive information about the study plots.

Site	Site id	Plot size (ha)	Age in 2017 (yrs)
Juan Enriquez	JE	1	22
Finca El Bejuco	FEB	1	22
Lindero Sur	LSUR	1	32
Tirimbina	TIR	1	35
LEP Secondary	LEPS	1	40
Cuatro Rios I	CR1	0.5	45
Cuatro Rios II	CR2	0.5	45
Selva Verde	SV	1	>100
LEP Primary	LEPP	1	>100

Table 2 – Stand-level mean, standard deviation (*SD*), coefficient of variation (CV), and range of lidar-derived canopy structural variables for the nine plots.

	Mean±*SD*	CV	Range
Canopy Height (m)	21.91 ± 2.31	10.6	17.21 - 25.08
spatial heterogeneity (m)	5.97 ± 1.56	26.2	4.11 - 8.53
Gap fraction (%)	1.12 ± 1.13	100.1	0.00 – 3.90
LAI (m^2/m^2)	7.24 ± 0.36	5.0	6.61 - 7.67
LAI understory (m^2/m^2)	1.28 ± 0.3	23.7	0.95 - 1.66
Shannon canopy index	3.33 ± 0.12	3.6	3.09 – 3.51
LAHV	145.61 ± 33.85	23.2	81.57 - 197.53

Figures legends

Figure 1. Study Area located in the Caribbean lowlands (50-220 m a.s.l.) of Heredia Province in northeastern Costa Rica. Land use classification based on satellite imagery from 2011 (Fagan et al., 2013).
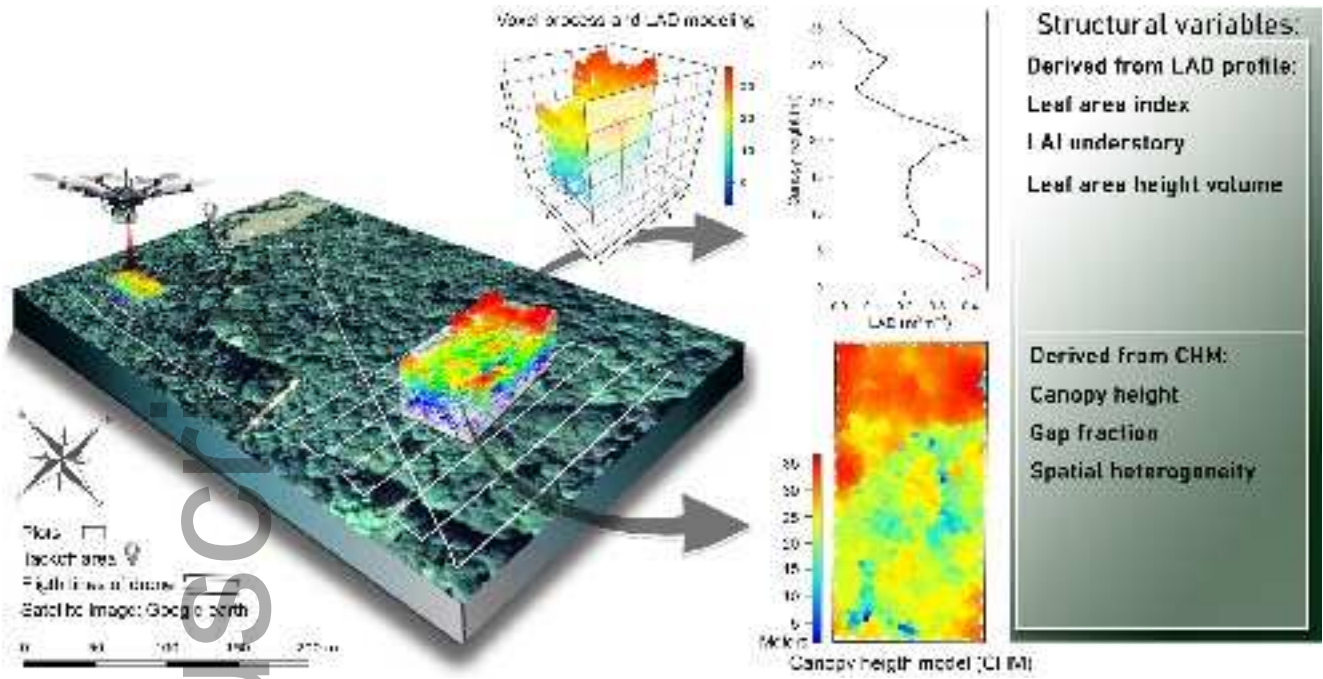
Figure 2. Flight plan of data collection and lidar-derived metrics. Example of a single flight in which two plots were overflown within the maximum flight time of 15 minutes for the DJI Matrice 600 Pro used to transport the sensor suite.

Figure 3. Lidar-derived leaf area density (LAD) profiles of nine plots in forests of different ages in Sarapiquí province, Costa Rica. The LAD is the area of leaves found in a unit of canopy volume. It can be seen as the decomposition of the leaf area index (LAI) among the vertical strata of the forest canopy.

Figure 4. Gap fraction, canopy spatial heterogeneity, and understory leaf area index ($LAI_{understory}$) as a function of forest age. The "*" point is an outlier not included in these regressions. Old-growth forests were assigned an age of 100 years.
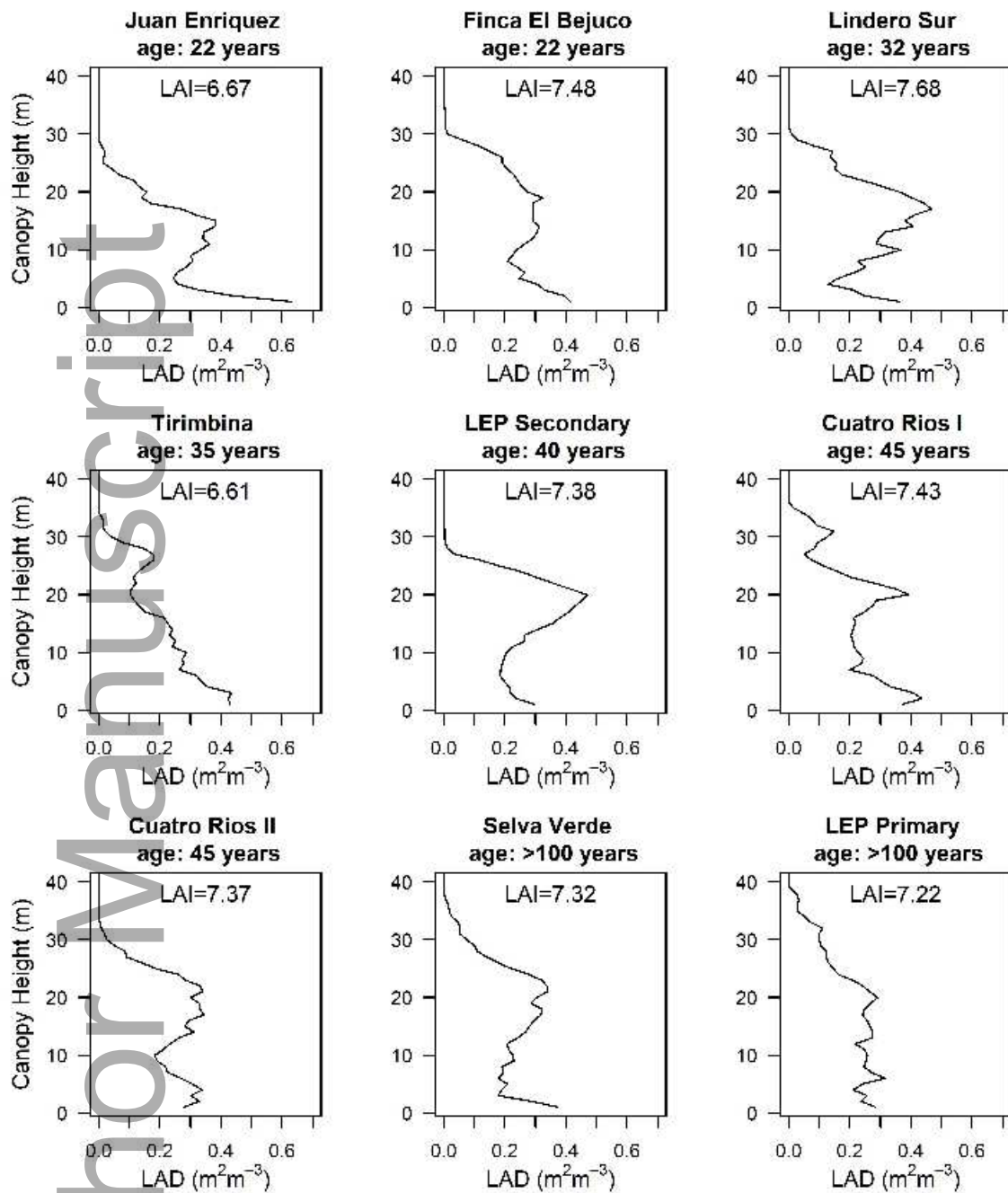
Figure 5. Field-derived aboveground dry wood biomass (ABG), lidar derived canopy height, and leaf area index (LAI) as a function of forest age. The parameter α is the asymptote of the model, β is the intercept of the model, and γ determines the rate of change. Old-growth forests were assigned an age of 100 years.

Figure 6. (A) Field-measured aboveground biomass (ABG) as a function of lidar-derived canopy height in nine forest plots in Sarapiquí, Costa Rica ($r^2 = 0.80$, $p = 0.001$, RMSE = 24.9, relative RMSE = 9.0%). Numbers in parentheses are the standard errors for each coefficient. (B) Leave-one-out cross-validation (LOOCV) of aboveground biomass. The solid line represents a 1:1 correspondence, and the dashed line (virtually indistinguishable from the solid line) is the linear regression fit between observed and leave-one-out predicted values ($obs_i = α + β·pred_i$). The values of α and β showed no significant difference from 0 and 1, respectively.
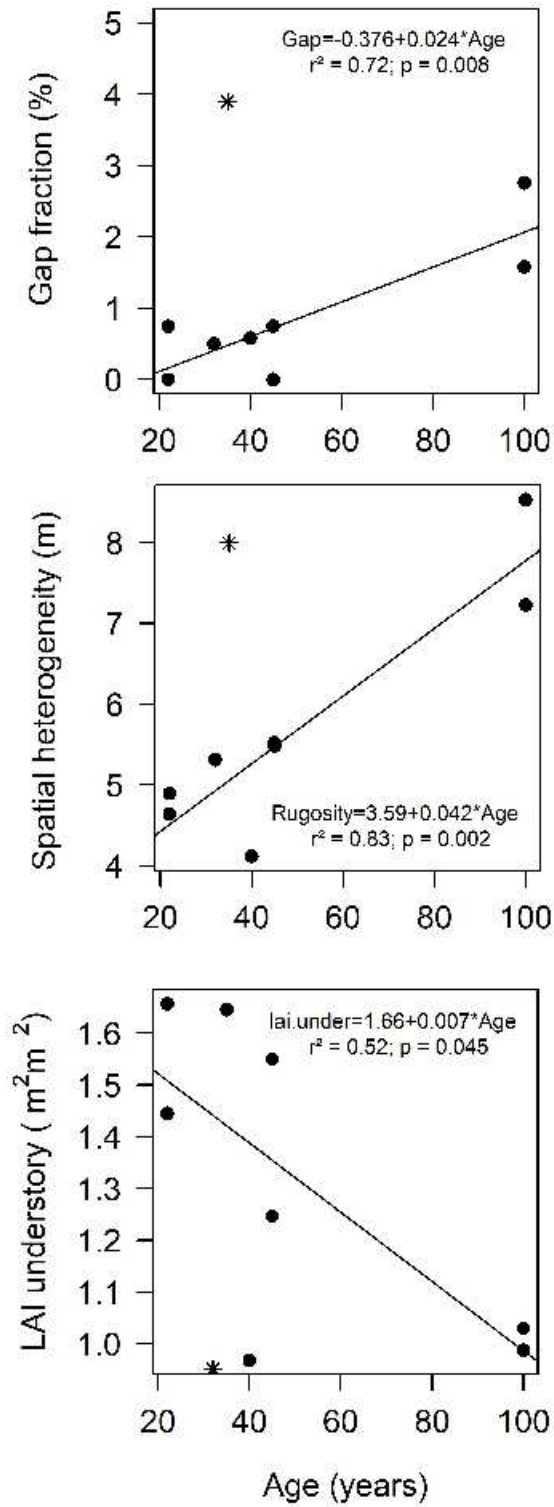
btp_12814_f1.jpg

btp_12814_f2.jpg
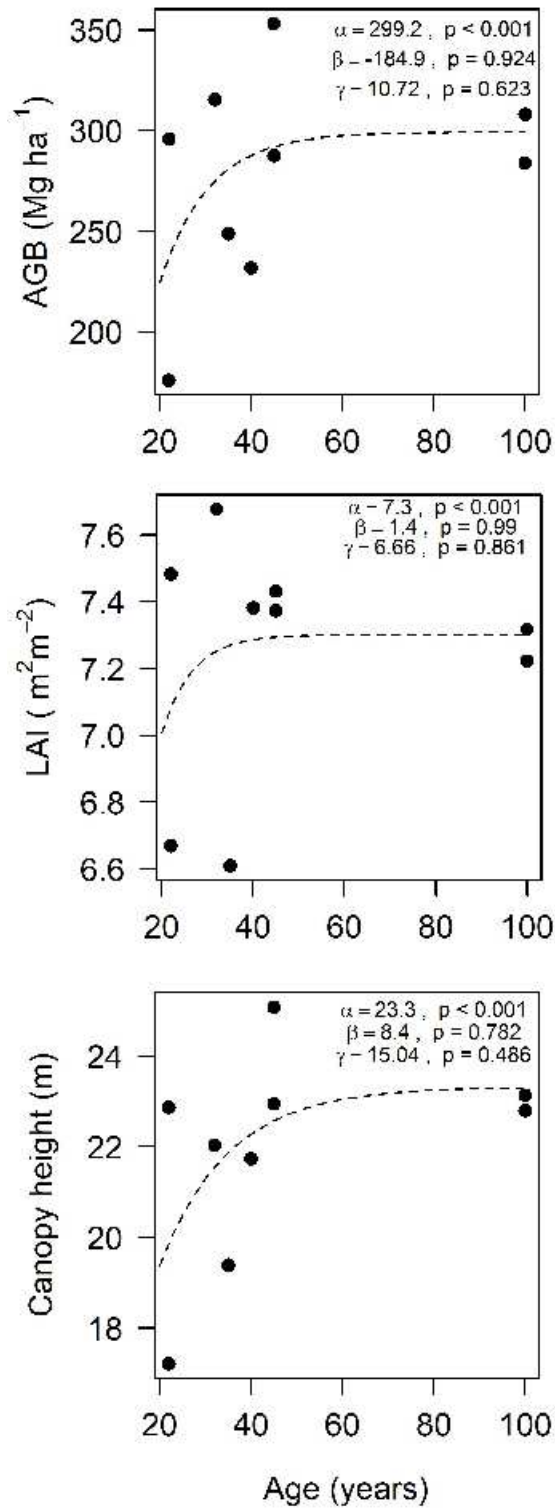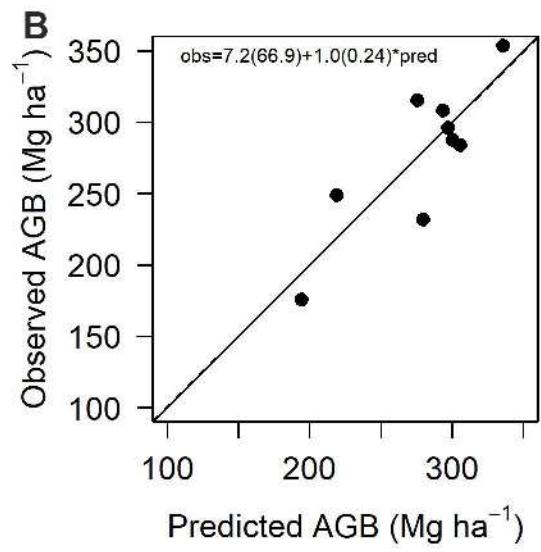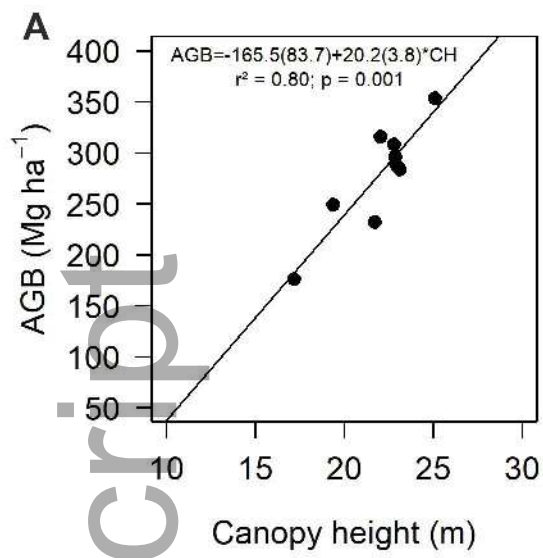
btp_12814_f3.jpeg

btp_12814_f4.jpeg

btp_12814_f5.jpeg

A AGB=-165.5(83.7)+20.2(3.8)*CH
$r^2 = 0.80$; $p = 0.001$

B obs=7.2(66.9)+1.0(0.24)*pred

btp_12814_f6.jpeg